REGULAR ARTICLE

blood advances

Synonymous *ADAMTS13* variants impact molecular characteristics and contribute to variability in active protein abundance

Katarzyna I. Jankowska,[1,*] Douglas Meyer,[1,*] David D. Holcomb,[1,*] Jacob Kames,[1] Nobuko Hamasaki-Katagiri,[1] Upendra K. Katneni,[1] Ryan C. Hunt,[1] Juan C. Ibla,[2] and Chava Kimchi-Sarfaty[1]

[1]OTAT/DPPT/HB in the Center for Biologics Evaluation and Research, US Food and Drug Administration, Silver Spring, MD; and [2]Department of Anesthesiology, Critical Care and Pain Medicine, Boston Children's Hospital and Harvard Medical School, Boston, MA

Key Points

- *ADAMTS13* sSNVs affect mRNA thermodynamic stability and may disturb mRNA-splicing sites.
- Synonymous variations may affect ADAMTS13 function and contribute to large variability in protein expression levels in healthy individuals.

The effects of synonymous single nucleotide variants (sSNVs) are often neglected because they do not alter protein primary structure. Nevertheless, there is growing evidence that synonymous variations may affect messenger RNA (mRNA) expression and protein conformation and activity, which may lead to protein deficiency and disease manifestations. Because there are >21 million possible sSNVs affecting the human genome, it is not feasible to experimentally validate the effect of each sSNV. Here, we report a comprehensive series of in silico analyses assessing sSNV impact on a specific gene. ADAMTS13 was chosen as a model for its large size, many previously reported sSNVs, and associated coagulopathy thrombotic thrombocytopenic purpura. Using various prediction tools of biomolecular characteristics, we evaluated all *ADAMTS13* sSNVs registered in the National Center for Biotechnology Information database of single nucleotide polymorphisms, including 357 neutral sSNVs and 19 sSNVs identified in patients with thrombotic thrombocytopenic purpura. We showed that some sSNVs change mRNA-folding energy/stability, disrupt mRNA splicing, disturb microRNA-binding sites, and alter synonymous codon or codon pair usage. Our findings highlight the importance of considering sSNVs when assessing the complex effects of *ADAMTS13* alleles, and our approach provides a generalizable framework to characterize sSNV impact in other genes and diseases.

Introduction

Although commonly assumed to be silent, synonymous single nucleotide variants (sSNVs) can cause protein deficiency or dysfunction severe enough to lead to disease[1-3] through various mechanisms. Synonymous variants may alter constitutive splice sites or activate cryptic splice sites, which can result in unstable messenger RNA (mRNA) or defective protein.[2] Synonymous changes may affect thermodynamic stability and secondary structure of mRNA or codon usage frequency, resulting in altered translational kinetics and cotranslational folding of a protein.[2,4] Recent studies suggest that intermittent ribosome stalling at key mRNA regulatory sites can affect protein abundance, folding, and even post-translational modifications, and the placement of certain stable structural elements within the mRNA sequence is not random.[2,5-7] Moreover, synonymous variants can disturb microRNA (miRNA)-binding sites in the coding sequence, which can lead to developmental defects and disease.[8]

Submitted 19 January 2022; accepted 1 June 2022; prepublished online on *Blood Advances* First Edition 6 June 2022; final version published online 21 September 2022. DOI 10.1182/bloodadvances.2022007065.

*K.I.J., D.M., and D.D.H. contributed equally to this study.

For data sharing, contact the corresponding author: Chava.Kimchi-Sarfaty@fda.hhs.gov.

The full-text version of this article contains a data supplement.

Synonymous variants can affect cytosine-guanine dinucleotide (CpG) sites, guanine-cytosine (GC) content, and codon usage biases, which may change the rate of translation due to ribosomal pausing.[9] Several studies found that ribosomal pauses relate to cotranslational folding of protein domains, which in turn determines the final protein conformation. Ultimately, by affecting gene regulatory signature, mRNA structure, and pre-mRNA processing, sSNVs can influence protein characteristics, including expression, function, and immunogenicity.[10-12]

ADAMTS13 (MIM:604134) controls the hemostatic function of von Willebrand factor (VWF; MIM: 613160) by splitting highly adhesive, ultra-large VWF multimers into smaller forms.[13] VWF is critical to the initial stage of thrombosis by tethering platelets to the endothelium at sites of vascular injury.[14] Regulation of VWF by ADAMTS13 prevents the spontaneous formation of platelet thrombi. Deficiency of ADAMTS13 increases VWF thrombogenic potential and may lead to microvascular thrombosis such as thrombotic thrombocytopenic purpura (TTP)[15,16] or congenital TTP, also known as Upshaw-Schulman syndrome (USS).[17] ADAMTS13 plays a crucial role in pediatric stroke pathogenesis,[18] and lower levels of ADAMTS13 have been associated with increased risks of coronary heart diseases and myocardial infarction.[19] Recently, clinical studies have shown the development of acquired TTP followed by COVID-19 infection and a strong association between low ADAMTS13 plasma levels and increased mortality in patients with COVID-19.[20]

The *ADAMTS13* gene is located on chromosome 9 and is ~37 kb long containing 29 exons. *ADAMTS13* mRNA is ~4 kb long and encodes 1427 amino acids.[21,22] This multidomain protein comprises a signal peptide, propeptide, metalloprotease, disintegrin-like domain, first thrombospondin type 1 repeat (TSP1), Cysteine-rich, and spacer domains. The distal C-terminus includes 7 additional TSP repeats and two CUB (C1r/C1s, urinary epidermal growth factor, bone morphogenetic protein) domains, that are unique for ADAMTS13.[23] The metalloprotease domain of ADAMTS13 modulates ADAMTS13 protein activity via cooperative binding to one Zn^{2+} ion and three Ca^{2+} ions.[24,25]

Among human *ADAMTS13* variants listed in a database of single nucleotide polymorphisms (dbSNP), ~200 disease-causative SNVs have been identified in patients with TTP,[26-28] all of which were non-synonymous and detected as haplotypes. Other SNVs may result in reduced plasma ADAMTS13 activity[29,30] and disrupted ADAMTS13–VWF interactions by changing untranslated regions (UTRs), splice regulatory regions, or the coding sequence. In addition, various truncated forms of ADAMTS13 are detectable in plasma, and several alternatively spliced mRNA variants have been characterized.[31-37]

Three genome-wide association studies (GWAS) revealed high heritability of ADAMTS13 levels (59.1%) and identified hundreds of non-synonymous and synonymous SNVs at the *ADAMTS13* locus that collectively explained ~20.0% of large ADAMTS13-level variation in healthy individuals.[30,38,39] Of 376 sSNVs registered in the National Center for Biotechnology Information dbSNP database, 357 sSNVs have been identified in healthy individuals, and 19 sSNVs have been identified in patients with USS[40] (supplemental Table 1). The impact of USS-associated sSNVs in the context of deleterious co-occurring mutations is currently unknown. Such sSNVs may have an additive negative impact, or they may help to enhance ADAMTS13 expression. For instance, the USS synonymous variant c.354G>A (rs28571612) yielded higher extracellular and intracellular ADAMTS13 expression levels and higher specific activity according to in vitro measurements.[10,41]

Due to limited data from GWAS and few experimental validations, the impact of specific sSNVs on ADAMTS13 function remains difficult to interpret. Nevertheless, prior studies show that variants in the *ADAMTS13* gene resulting in deficient ADAMTS13 activity may disturb VWF activity and lead to coagulopathies such as USS.[15] Understanding the factors that contribute to ADAMTS13 expression and disturb normal protein activity could help reduce diagnostic errors, prevent TTP development, and improve treatment.

Considering the substantial number of observed synonymous variants, comprehensive experimental verification is difficult to perform. Use of computational predictors and modeling can reveal sSNVs that are most likely to affect protein function and disease.[3] This approach can help focus experimental studies on a smaller subset of synonymous variants most likely to have a detectable impact on protein characteristics.

To better understand the contributions sSNVs may make to protein biogenesis using *ADAMTS13* as a model, we performed comprehensive in silico analysis of all known *ADAMT13* sSNVs. Our results highlight sSNVs that may alter mRNA splicing, change mRNA-folding energy, disturb miRNA-binding sites, and affect synonymous codon usage. This in silico analysis provides a generalizable approach to characterize the effects of sSNVs influencing other genes and diseases.

Methods

ADAMTS13 sSNV selection

The *ADAMT13* variants were obtained from the National Center for Biotechnology Information dbSNP database (https://www.ncbi.nlm.nih.gov/SNP/snp_ref.cgi?locusId=11093; GRCh38.p7). All SNVs from *ADAMTS13* were filtered to include only synonymous variants in the open reading frame. Of >1000 SNVs, all 376 sSNVs were selected for further evaluation and compared with the wild-type (WT) *ADAMTS13* (NM_139025). All sSNVs obtained from the dbSNP (supplemental Excel Worksheet 1) include 357 neutral variants and 19 sSNVs that were identified in patients with USS (USS variants). Although the USS variants are labeled as "being-likely" to cause the disease, this has not yet been confirmed. To our knowledge, there are no confirmed disease-associated *ADAMTS13* sSNVs.

In silico studies of *ADAMTS13* sSNVs

Determination of mRNA-folding energy, stability, and structure were performed by using mFold,[42] NUPACK,[43] kineFold,[44] remuRNA,[45] and RNAFold.[46] Splicing impact of *ADAMTS13* sSNVs was evaluated by using MaxEntScan (MES),[47] NNsplice,[48] SpliceSiteFinder-like,[49] and GeneSplicer.[50]

Evaluation of miRNA-binding sites within the coding region of *ADAMTS13* sSNVs was performed by using miRDB,[51,52] PaccmitCDS,[53,54] and TargetScan.[55] Relative synonymous codon usage (RSCU) and relative synonyms bicodon usage (RSBCU) were calculated as previously described.[43,56] Codon pair score without natural log (CPS),[57] rare codon (RC) enrichment,[58] and codon adaptation index (W)[56] were computed as previously described. RC

clustering for *ADAMTS13* sSNVs was computed by using %MinMax.[59] Protein folding energy was estimated by using a coarse-grained cotranslational folding energy model.[58]

Complete descriptions of the in silico methods are given in the supplemental Methods, and data produced are provided in Excel Worksheets 1 to 3.

Results

Synonymous mutation patterns in *ADAMTS13*

A total of 376 naturally occurring sSNVs of *ADAMTS13,* including 357 from a healthy population and 19 from patients with USS, were identified in the dbSNP; they affect almost 9% of nucleotides in the mRNA of *ADAMTS13* and >26% of codons. Most sSNVs have been identified in exon 25. Many sSNVs have been found within the metalloprotease domain and C-terminal region of *ADAMTS13*, in exons 24 to 29, which encode the TSP7-8 and CUB1-2 domains (Figure 2A).

The distribution of base changes across the sSNVs of *ADAMTS13* shows that the most frequently occurring base changes were C>T and G>A, agreeing with prior studies reporting synonymous base pair change frequencies.[60,61] Of 19 USS variants, 11 were identified within the TSP2-8 and CUB1 domains. Accounting for exon length, sSNVs most frequently affected exons 1, 5, 8, and 25 (~11% sSNV per exon length) that encoded signal peptide, metalloprotease, and T8 domains, respectively (Figure 2B). In contrast, sSNVs were rarely found in exons 2 to 4, 9, and 23 encoding the propeptide, metalloprotease, disintegrin-like, and T6 domains, respectively (~6% sSNV per exon length). The most frequent types of ADAMTS13 sSNVs, C>T and G>A (Figure 2C), lower GC content.

Most identified *ADAMTS13* sSNVs are very rare, with a frequency <0.001.[62,63] The 12 most frequently occurring sSNVs are listed in Table 1. Interestingly, 6 of these variants were identified in patients with USS. The frequencies of all 376 sSNVs are included in supplemental Excel Worksheet 1.

sSNVs may affect RNA-folding energy and secondary structure

We next evaluated RNA-folding energy of *ADAMTS13* sSNVs. Such changes may affect antigen and activity levels of the protein. Experimental measurement of mRNA structure remains a challenge, especially to a degree of sensitivity that could detect structural differences resulting from single nucleotide changes.[64] However, algorithms such as mFold,[42] kineFold,[44] remuRNA,[45] or NUPAC[43] can evaluate the stability of mRNA fragments by calculating Gibbs free energy (ΔG) of possible secondary structures.[1]

Using these 4 algorithms, we calculated ΔΔG ($\Delta G_{variant} - \Delta G_{wildtype}$) for all *ADAMTS13* sSNVs (Figure 3A; supplemental Figure 1A). According to at least one algorithm, 67 sSNVs caused significantly altered folding energy compared with WT ($P < .05$) (Figure 3B-C). (The supplemental Methods provides a description of *P* value

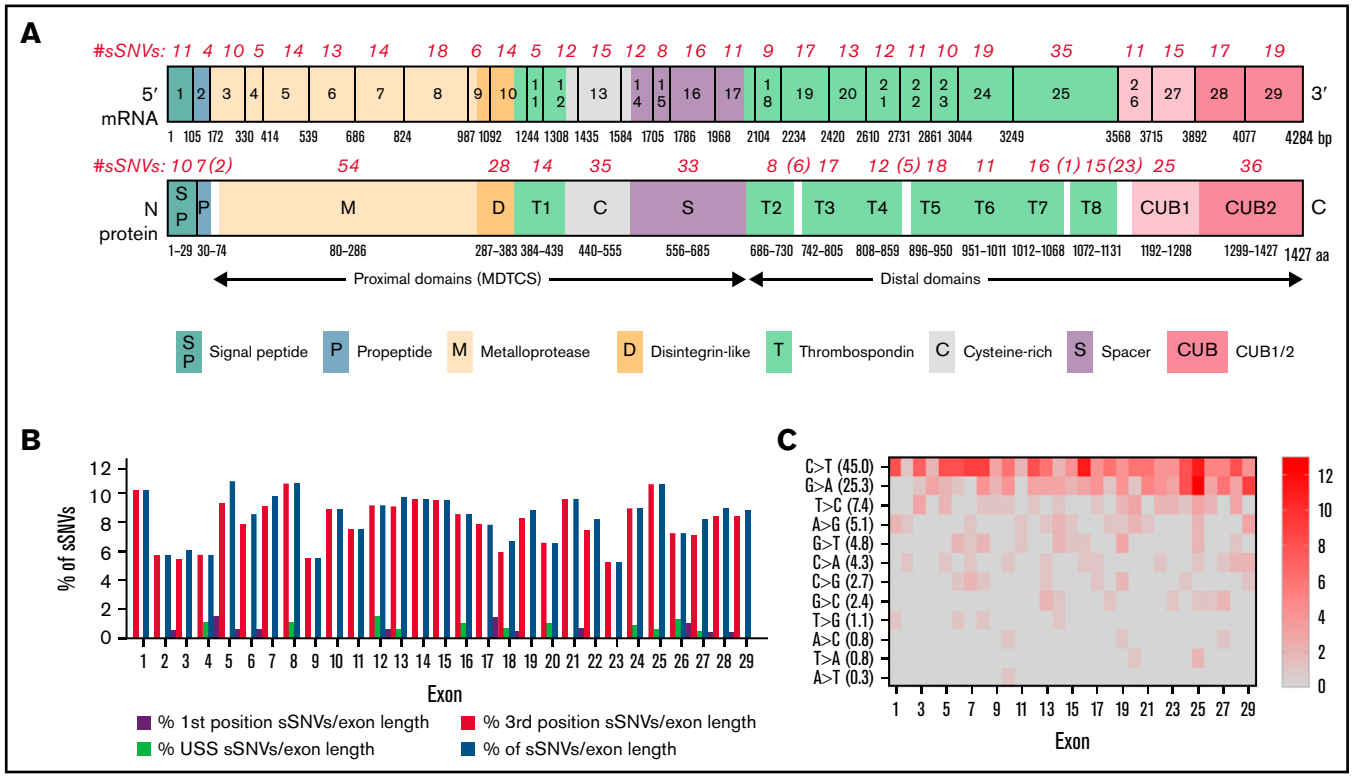

Figure 1. *ADAMTS13* synonymous variant characteristics. (A) Schematic diagram of *ADAMTS13* exons and encoded protein domains with the number of sSNVs in each exon and domain (in italic red). (B) Proportion of 376 variants present in first codon position (solid red) or in third codon position (red outline). Proportion of sSNVs found in patients with USS (yellow). Proportion of variants present in each exon, normalized by exon length (gray). (C) Distribution of 12 possible nucleotide substitutions of synonymous mutations across *ADAMTS13* exons and the percentage of variants with given nucleotide substitution provided in parentheses.

Table 1. Summary of most frequently occurring synonymous variants of *ADAMTS13*

sSNV	ID	Exon	Domain	AA #	AA	USS variant	Frequency	Source
1716G>A	rs3124768	15	S	572	T		0.488347	HapMap
420T>C	rs3118667	5	M	140	A		0.45704	ALFA
4221C>A	rs1055432	29	CUB2	1407	T		0.316033	ALFA
354G>A	rs28571612	4	M	118	P	Y	0.078803	ALFA
3108G>A	rs34934621	24	T7	1036	S	Y	0.047011	ALFA
2508T>C	rs36221472	20	T4	836	D	Y	0.006502	ALFA
357C>T	rs147563206	4	M	119	S		0.002774	ALFA
546C>T	rs148849381	6	M	182	D		0.002196	1000Genomes
3150G>A	rs36222579	24	T7	1050	V		0.001962	ALFA
1551G>C	rs148472763	13	C	517	G	Y	0.001879	ALFA
936C>T	rs36219562	8	D	312	R	Y	0.001074	ALFA
2217C>T	rs144178018	18	T2/T3	739	L	Y	0.001074	ALFA

Briefly summarizes 12 sSNVs of *ADAMTS13* with relatively high frequency (>0.001) according to the Allele Frequency Aggregator project (ALFA), the HapMap Project (HapMap), or the 1000 Genomes Project (1000Genomes). A complete description of other sSNV frequencies is provided in supplemental Excel Worksheet 1. AA, amino acid; C, cysteine-rich; D, disintegrin-like; M, metalloproteinase; S, spacer.

computation, and supplemental Excel Worksheet 1 provides the *P* values). Although the sSNVs generally resulted in increased ΔG and were predicted to cause structural instability, we found some sSNVs, particularly in exons 1, 6, 14, and 19, which caused significant decreases in ΔG and thus more stable mRNA structures (Figure 3B). Others have proposed that thermodynamically stable mRNA secondary structures should have a selective advantage.[65]

The synonymous variant c.999G>A results in the highest positive ΔΔG by mFold and remuRNA and consistently positive ΔΔG by the other 2 tools. Variants c.1521G>A and c.2385G>A displayed significantly positive ΔΔG by mFold and kineFold. The lowest negative ΔΔG predicted by mFold was found in variant c.2067C>A. This variant had significantly negative ΔΔG predicted by kineFold and remuRNA and was the only sSNV with significantly negative ΔG calculated by 3 tools. Variant c.1462C>A displayed the lowest negative ΔΔG calculated by NUPAC and significantly negative ΔΔG calculated by kineFold. Finally, the variant c.4041C>T within exon 28 was predicted to significantly decrease stability according to mFold and kineFold (Figure 3C). None of the 19 USS variants (supplemental Figure 1B) and 2 of the 12 high-frequency variants (supplemental Figure 1C) yielded significant ΔΔG.

We next predicted full-length mRNA secondary structure of highly frequent variants (Table 1) and from variants resulting in most positive (c.999G>A) and most negative (c.1462C>A) ΔΔG by RNAfold. ΔG and the optimal mRNA secondary structure of either sSNV differ from those of WT *ADAMTS13* mRNA (Figure 3D; supplemental Figure 2; supplemental Table 2).

We observed moderate correlations between ΔΔG for the 4 algorithms used, with the strongest correlation between mFold and remuRNA, whereas kineFold exhibited the weakest correlations among all 4 (Figure 3E). Although few variants were predicted to significantly affect ΔΔG by multiple algorithms, the direction of the impact (increase or decrease) was generally consistent across the different algorithms (Figure 3C).

In summary, numerous sSNVs may affect *ADAMTS13* mRNA thermodynamic stability, and these alterations in mRNA secondary structure may have strong effects on gene function and play an important role in disease onset and progression.[7,66]

Most *ADAMTS13* sSNVs negatively affect CpG sites and decrease GC content

We next examined ADAMTS13 sSNVs for their impact on GC content and CpG sites.

The majority of ADAMTS13 sSNVs reduce GC content (Figure 4A), especially in exons 4, 12, 16, 21, and 24. Of the 376 ADAMTS13 sSNVs, 144 affected CpG sites (Figure 4B). Only 55 sSNVs increased GC content, and 31 sSNVs resulted in a creation of new CpG sites (Figure 4C). The sSNV 33T>G may create a new CpG site in exon 1, potentially affecting the DNA methylation state. Previous studies have shown that CpG sites are frequently methylated[9,67] and that methylation in the first exon suppresses gene expression,[68] suggesting that this variant may influence ADAMTS13 expression.

As indicators of structural stability, observations of moderate correlations between ΔG and GC content of both WT and variant sequences were not surprising. However, weak correlations were observed between ΔΔG and ΔGC content (Figure 4D).

sSNVs may affect pre-mRNA splicing and miRNA-binding sites

We next examined the possible impact of sSNVs on splicing and miRNA regulation of ADAMTS13 (Figure 2A-B; supplemental Excel Worksheets 2-3), which are 2 common mechanisms by which sSNVs can affect protein structure.[2,6] We identified 7 variants predicted to affect constitutive splice donor or acceptor sites (Figure 5A), which might result in exon skipping or intron retention. In addition, 36 variants were identified that may activate cryptic splice sites, and although these cryptic sites are not associated with previously characterized ADAMTS13 splice isoforms, they may still limit expression of constitutive ADAMTS13 transcript. Seven variants were predicted to affect special cryptic sites, which are associated with alternative splice products of ADAMTS13 (NM_139026

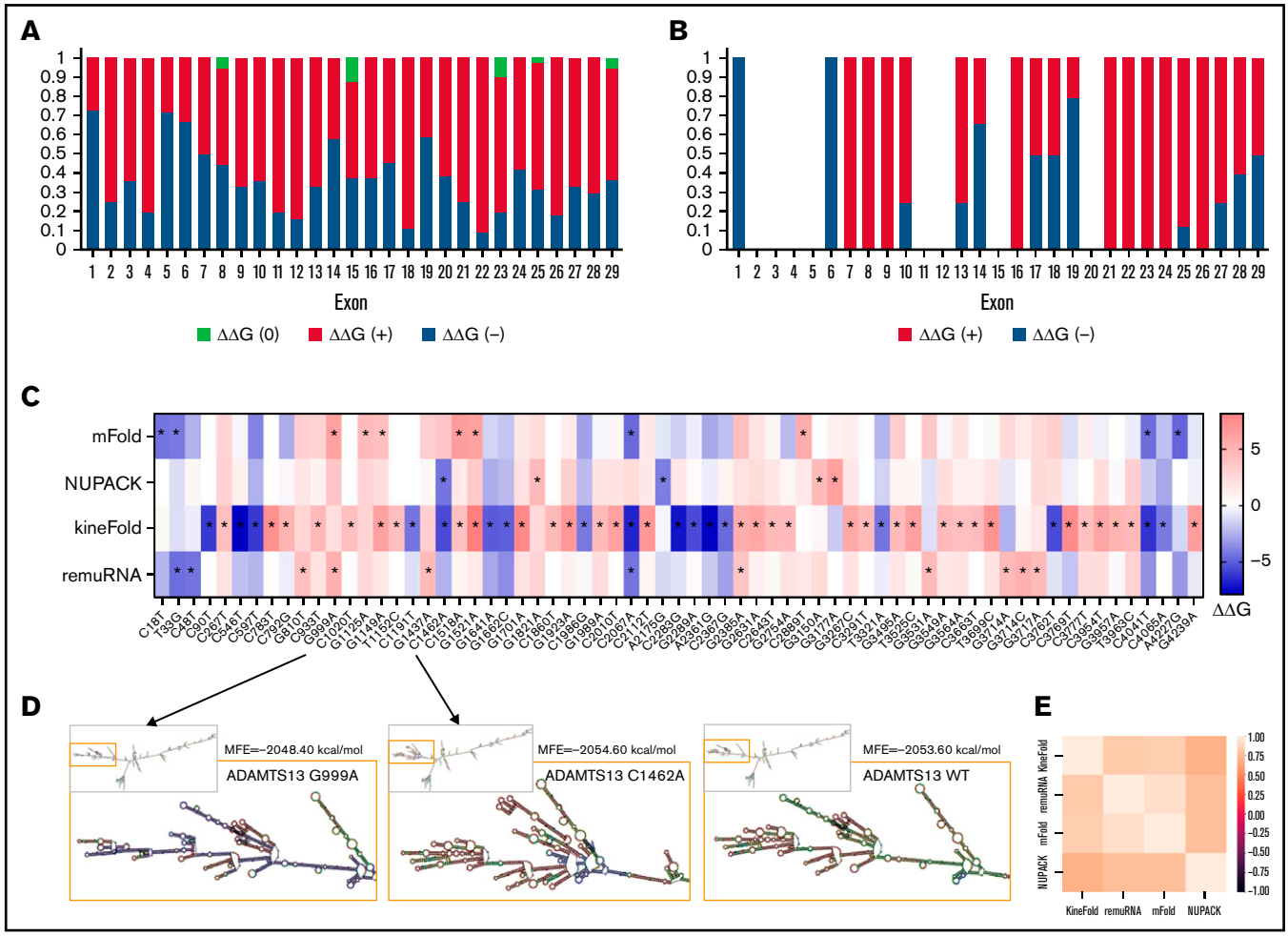

Figure 2. *ADAMTS13* sSNVs affect the folding energy and mRNA secondary structure. (A) Stacked column plot that displays the proportions of all sSNVs in each exon that decrease ΔΔG (–, blue), increase ΔΔG (+, red), or do not change ΔΔG (0, white) based on average value obtained from all 4 algorithms (see Methods). (B) Stacked column plot that displays the ratio of significantly different sSNVs (P values $< .05$) in each exon. (C) Synonymous *ADAMTS13* variants with significantly (*) different ΔΔG compared with WT as predicted by at least one algorithm ($P < .05$). (D) Optimal full-length mRNA secondary structure of *ADAMTS13* predicted by RNAFold for variants 999G>A and 1462C>A compared with WT *ADAMTS13*. (E) Correlation between the ΔΔG values obtained by mFold, remuRNA, KineFold, and NUPAC for all 376 *ADAMTS13* sSNVs. Differences considered significant in which $P < .05$ (see supplemental Methods for description of P value computation and supplemental Excel File 1 for P values).

and NM_139027). Five of these variants weakened special cryptic sites, potentially resulting in decreased production of alternative transcripts. The c.909C>T variant was predicted to strengthen the special exon 8 acceptor site, potentially decreasing primary transcript expression in favor of the NM_139026 transcript. The c.918C>T variant was predicted to strengthen (NNsplice) and weaken (MES) the special exon 8 acceptor site, making it difficult to predict this variant's impact. Variants predicted to affect splicing were found in 15 different exons and influence positions that encode several protein domains, including metalloprotease domain (10 sSNVs), disintegrin-like domain (15 sSNVs), Cysteine-rich domain (2 sSNVs), spacer domain (5 sSNVs), and TSP repeats (10 sSNVs) (Figure 5A; supplemental Table 3).

To further validate predictions of splice impact, we used additional tools (SpliceSiteFinder-like and GeneSplicer) for variants predicted to affect splicing by MES or NNsplice. For variants predicted to affect constitutive splice sites, limited agreement was found between the tools used (Figure 5C). However, we found 5 variants predicted to affect cryptic splice sites with complete agreement between 4 splicing tools and 4 additional variants with agreement between 3 splicing tools (Figure 5D).

Because *ADAMTS13* sSNVs may affect miRNA-binding sites and cause translational suppression or protein degradation,[69] we next examined variants for their likelihood to affect miRNA-*ADAMTS13* binding based on Paccmit-CDS, TargetScan, and miRDB. We found 9 variants predicted to affect miRNA-binding sites by all 3 tools (Figure 5B). These 9 variants resulted in gain of binding sites for 10 different miRNA species and loss of binding sites for 4 miRNA species.

Because TargetScan and miRDB are tools primarily used to assess miRNA binding in 3′UTR, we expected to see some disagreement between these tools and Paccmit-CDS, which was specifically developed to assess miRNA binding to mRNA-coding regions. We

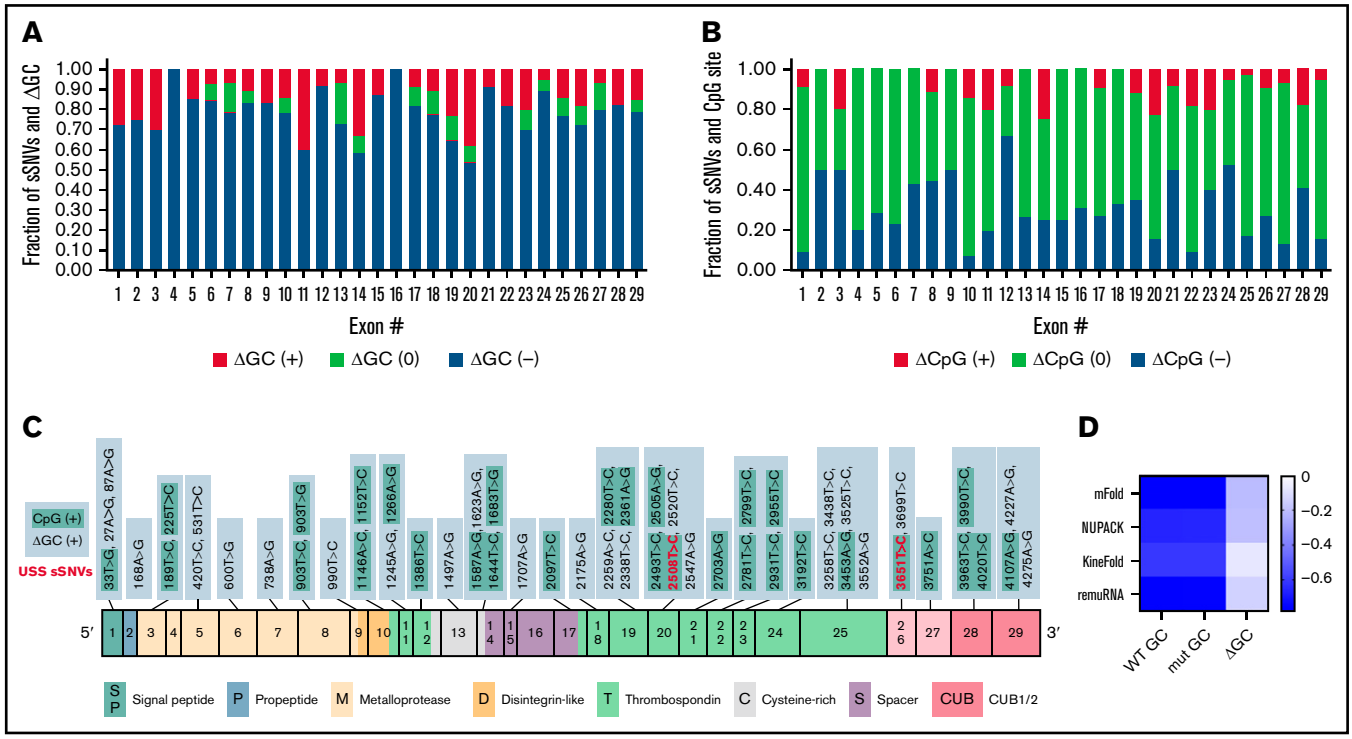

Figure 3. Synonymous *ADAMTS13* variants affect GC content and CpG sites. (A) Proportion of sSNVs in each exon that increase GC content (red), decrease GC content (blue), or do not affect GC content (green). (B) Proportion of sSNVs in each exon that increase CpG (red), decrease CpG (blue), or do not affect CpG (green). (C) Fifty-five synonymous variants that exhibit ΔGC >0 and 31 sSNVs that created new CpG site (positive CpG) across ADAMTS13 exons. (D) Correlation between folding energy and GC content in variant and WT *ADAMTS13*. USS variants are shown in red.

found substantially higher overlap between TargetScan and other algorithms when using extended seed (nucleotides 2-8 of the miRNA) rather than nucleotides 1 to 7 as seed sequences (Table 2; supplemental Table 4; supplemental Figure 3); thus, the TargetScan values resulted from using bp 2 to 8 (Figure 5E; Table 2).

Paccmit-CDS predicted gain/loss of 3408 miRNA-binding sites resulting from sSNVs. Of these 3408 affected miRNA-binding sites, 14 were predicted by TargetScan and miRDB (Figure 5B; Table 2), and 186 were predicted by TargetScan (Figure 5E). From these predicted miRNAs, miR-221-5p and miR-1248 were shown to be expressed in liver cells,[70,71] where ADAMTS13 is predominantly expressed.[72] Further confirming its relevance to the liver, miR-221 displayed upregulation in liver fibrosis[73] and promoted human hepatocellular carcinoma migration.[74]

Some sSNVs significantly affect the codon usage bias

We next evaluated how sSNVs could change *ADAMTS13* synonymous codon preference. Here, *P* values <.05 were considered significant.

A total of 83 sSNVs exhibited significantly different codon usage or codon pair usage based on RSCU and RSBCU values, respectively (Figure 6A; supplemental Figure 4). From this group, 22 sSNVs displayed significantly different codon adaptation index (ΔW) (Figure 6B). *ADAMTS13* sSNVs commonly inserted RCs (supplemental Table 5), which are expected to decrease translation rate. Among them, variants c.360G>A, c.451C>T, c.1125G>A, c.1557G>A, c.2754G>A, c.3501G>A, c.3810C>A, and c.4185G>A led to decreases in codon usage metrics. Only 7 synonymous variants significantly increased indices of codon usage (supplemental Figure 4).

We also calculated changes in CPS for sSNVs of *ADAMTS13* to measure the impact of codon pair usage while controlling for codon usage. Forty-one sSNVs exhibited significantly different CPS values (Figure 6C). Three sSNVs (c.138G>T, c.225 T>C, and c.1989G>A) exhibited the largest decrease in CPS values. Only two sSNVs (c.738A>G and c.2703A>G) resulted in increased CPS for both affected codon pairs, although the increase was only significant for the 5′ codon pair. As expected, ΔRSCU showed a strong linear correlation with Δ%MinMax (supplemental Figure 5A), and we found a stronger correlation between CPS and RSBCU for 3′ codon pair than 5′ codon pair (supplemental Figure 5B-C). Next, we computed rare and common codon clustering for *ADAMTS13* sSNVs using %MinMax.[75] Of these, 31 variants resulted in significantly decreased %MinMax, and 5 resulted in significantly increased %MinMax (Figure 6D). Variants that decrease %MinMax imply the insertion of RCs, which can reduce local translation rate[75]; variants that increase %MinMax imply the loss of RCs, which may be necessary for proper cotranslational folding.[76]

In addition, we investigated RC enrichment at positions of *ADAMTS13* sSNVs and identified several loci with significant RC enrichment (supplemental Figure 6). RCs may inhibit translational initiation or slow translation elongation, which in turn can promote mRNA degradation and even affect protein folding.[77] The highest

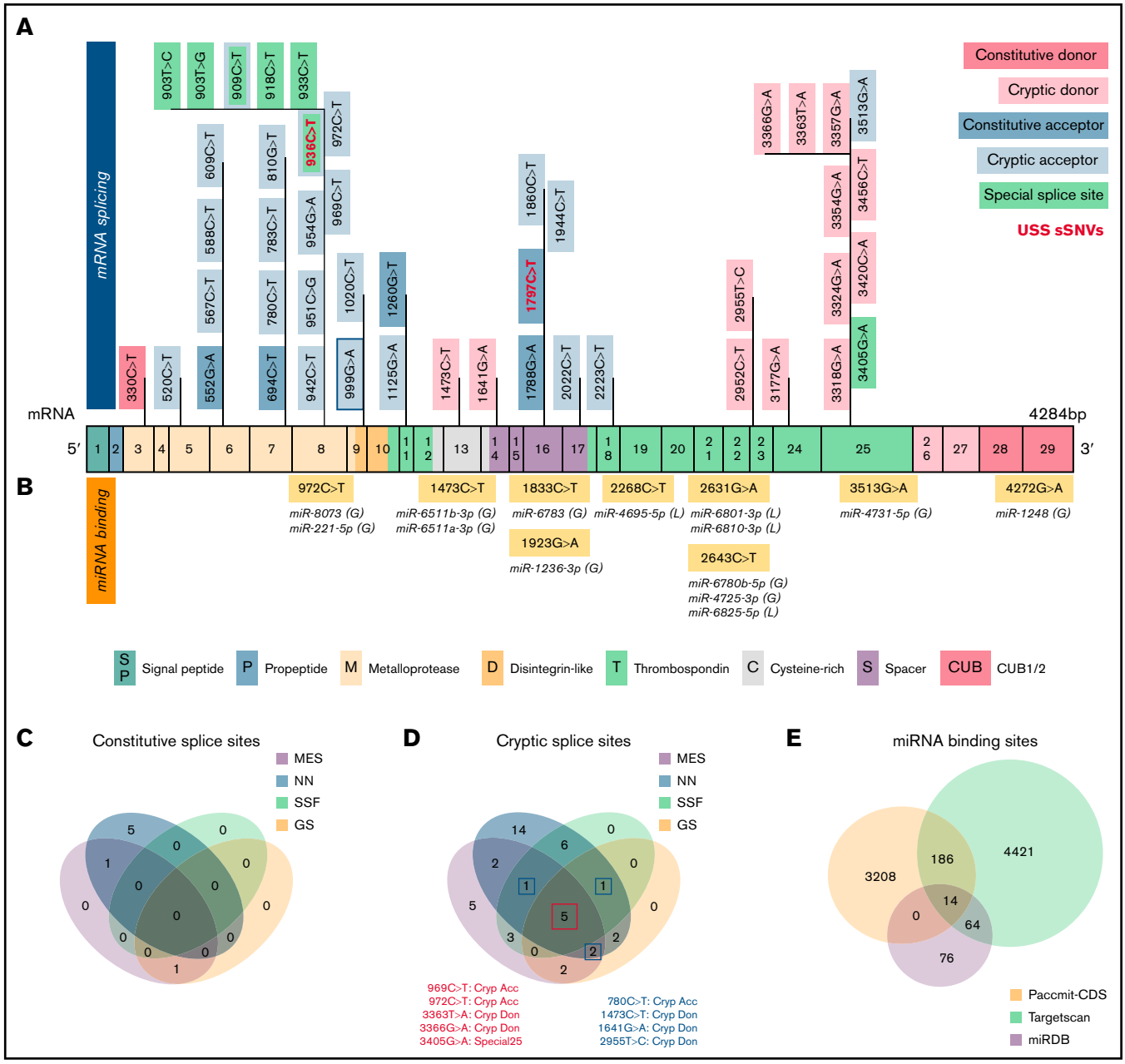

Figure 4. Synonymous variants may affect splicing and miRNA-binding sites within *ADAMTS13*. (A) ADAMTS13 sSNVs that were predicted to affect splice sites across *ADAMTS13* exons and encoded protein domains. Exons are colored consistent with the protein domain(s) they encode. sSNVs that were predicted to affect constitutive donors are highlighted in dark pink, and those predicted to affect constitutive acceptors are highlighted in dark blue. Variants predicted to affect cryptic donors are highlighted in light pink, and those predicted to affect cryptic acceptors are highlighted in light blue. Variants predicted to affect special case exon 8 acceptor or exon 25 donor are colored green. USS variants are shown in red. (B) Variants predicted to affect miRNA-binding sites according to Paccmit-CDS, TargetScan, and miRDB. Consistency of splice affects predictions between MES, NNsplice (NN), SpliceSiteFinder-like (SSF), and GeneSplicer (GS) splice prediction tools for constitutive splice sites (C) and for cryptic and special case cryptic splice sites (D). (E) Venn diagram displays numbers of *ADAMTS13* sSNVs that affect miRNA-binding sites as predicted by Paccmit-CDS, TargetScan, and miRDB. Acc, acceptor; C, cysteine-rich; Cryp, cryptic; D, disintegrin-like; Don, donor; M, metalloproteinase; P, propeptide; T1-T8, thrombospondin repeats 1-8; S, spacer; CUB (C1r/C1s, urinary epidermal growth factor, bone morphogenetic protein); SP, signal peptide.

increase in RC values were observed at positions 1551, 2439, 2448, and 3684 in exons 13, 20, 20, and 26, respectively. Synonymous variations in these positions may affect ADAMTS13 translational rate and disturb protein folding.

When comparing variants that significantly affect RSCU, RSBCU, W, and %MinMax, we identified 10 sSNVs located in multiple different exons (Figure 6E) that significantly affect all parameters. We found 3 of these variants also significantly

Table 2. Synonymous *ADAMTS13* variants predicted to affect miRNA-binding sites

sSNV	ID	Exon	Domain	AA #	AA	miRNA	Effect
972C>T	rs782268976	8	D	324	F	miR-8073	Gain
972C>T	rs782268976	8	D	324	F	miR-221-5p	Gain
1473C>T	rs140501683	13	C	479	G	miR-6511b-3p	Gain
1473C>T	rs140501683	13	C	479	G	miR-6511a-3p	Gain
1833C>T	rs1373112883	16	S	611	I	miR-6783-5p	Gain
1923G>A	rs977615435	16	S	641	E	miR-1236-3p	Gain
2268C>T (*)	rs781923426	19	T3	756	A	miR-4695-5p	Loss
2631G>A (*)	rs782772606	21	T4/T5	877	G	miR-6810-3p	Loss
2631G>A	rs782772606	21	T4/T5	877	G	miR-6801-3p	Loss
2643C>T (*)	rs1260442569	21	T4/T5	881	P	miR-6780b-5p	Gain
2643C>T (*)	rs1260442569	21	T4/T5	877	G	miR-4725-3p	Gain
2643C>T (*)	rs1260442569	21	T4/T5	877	G	miR-6825-5p	Loss
3513G>A	rs368634068	25	T8/CUB1	1171	P	miR-4731-5p	Gain
4272G>A	rs938453395	29	CUB2	1409	Q	miR-1248	Gain

All 3 tools (miRDB, PACCMIT, and TargetScan nucleotides 2-8 seed) predict 9 sSNVs to affect 14 miRNA-binding sites within the coding region of WT ADAMTS13. Asterisks highlight variants also predicted to affect miRNA binding. AA, amino acid; C, cysteine-rich; D, disintegrin-like; S, spacer.

affected RC but we found no sSNVs that also significantly affect CPS (supplemental Figure 7).

sSNVs may affect mRNA regions encoding the ADAMTS13 active site and metal-binding domains and its protein structure

Next, we investigated the regions essential for *ADAMTS13* functionality to assess their vulnerability to sSNVs. Detailed crystal structure evaluation of ADAMT13 proximal domain MDTCS[25] compared with identified sSNV positions revealed 13 sSNVs affecting loci critical for metal binding and protein activity (Figure 7A-C; Table 3). C.564C>T affected a codon directly involved in Ca^{2+} binding (Figure 7B). Another variant, c.1980G>A, is localized within the loop 660-672 that is essential in interaction with VWF[78,79] and/or CUB domains relevant to "closed" ADAMTS13 conformation (Figure 7C).[80]

Nevertheless, 4 of these 13 sSNVs were predicted to affect mRNA splicing: c.546C>T, c.552G>A, c.567C>T, and c.834G>T (Figure 5A). Two were predicted to affect miRNA-binding sites: c.1833C>T and c.1980G>A (Table 2). Two variants significantly affected mRNA folding energy (supplemental Figure 8A).

CUB1 domain amino acids Cys1254 and Cys1275 are essential for proper secretion and proteolytic activity of ADAMTS13,[81] suggesting relevance of c.3762C>T and c.3825C>T variants. Furthermore, 16 additional sSNVs were identified in codons encoding cysteine, whose disulfide bonds stabilize the overall structure of ADAMTS13, and 42 sSNVs were identified in codons encoding proline, which introduces rigid turns into the peptide chain and sets α-helix and β-sheet borders.[82] Because proline and cysteine substantially influence protein structure, we expect more severe consequences from variants affecting proline or cysteine codons than from variants affecting other codons. Variants affecting cysteine codons did not significantly influence mRNA stability or codon usage (supplemental Figure 8B). Interestingly, based on amino acid frequency in ADAMTS13, neutral sSNVs affecting cysteine codons were 15% less frequent than expected (supplemental Table 6).

Proline codons, in addition to those encoding alanine and threonine, were among the most frequently affected codons by sSNVs of *ADAMTS13* (Figure 7D; supplemental Table 6). Proline codons are often affected by sSNVs in signal peptide, propeptide, and disintegrin-like domains (supplemental Figure 9). Several variants affecting proline codons were predicted to influence other examined parameters (supplemental Figure 8C). Seven variants may affect splicing (Figure 6), and 2 may affect miRNA binding (Table 2).

In addition, threonine, alanine, and proline codons were more commonly affected by *ADAMTS13* sSNVs, whereas tyrosine codons were less commonly affected by sSNVs than was expected (supplemental Table 6; supplemental Figure 9). Synonymous mutation in leucine codons dominate in metalloprotease and CUB domains, whereas sSNVs in neutral alanine codons were seen most frequently in thrombospondin domains. USS variants mostly encode leucine valine and serine codons (Figure 7D; supplemental Figure 9H).

Finally, because changes in translation kinetics may affect cotranslational folding, we calculated ADAMTS13 folding energy of the nascent protein chain. We identified three variants (c.3150G>A, c.3177G>A, and c.2338T>C) downstream from areas of large changes in cotranslational folding energy (Table 4) and which change RSCU or RSBCU. Together, this implies these variants have the greatest potential impact on protein secondary structure.

Discussion

Although most identified *ADAMTS13* sSNVs are very rare, common sSNVs mainly coexist as haplotypes, making it very challenging to find individuals with a single sSNV to evaluate its effect. Conversely, cost and complexity remain substantial obstacles for comprehensive characterization of sSNVs affecting protein properties and disease states in vitro. Our in silico analysis of biomolecular characteristics of ADAMTS13 reveals a powerful opportunity for high-throughput

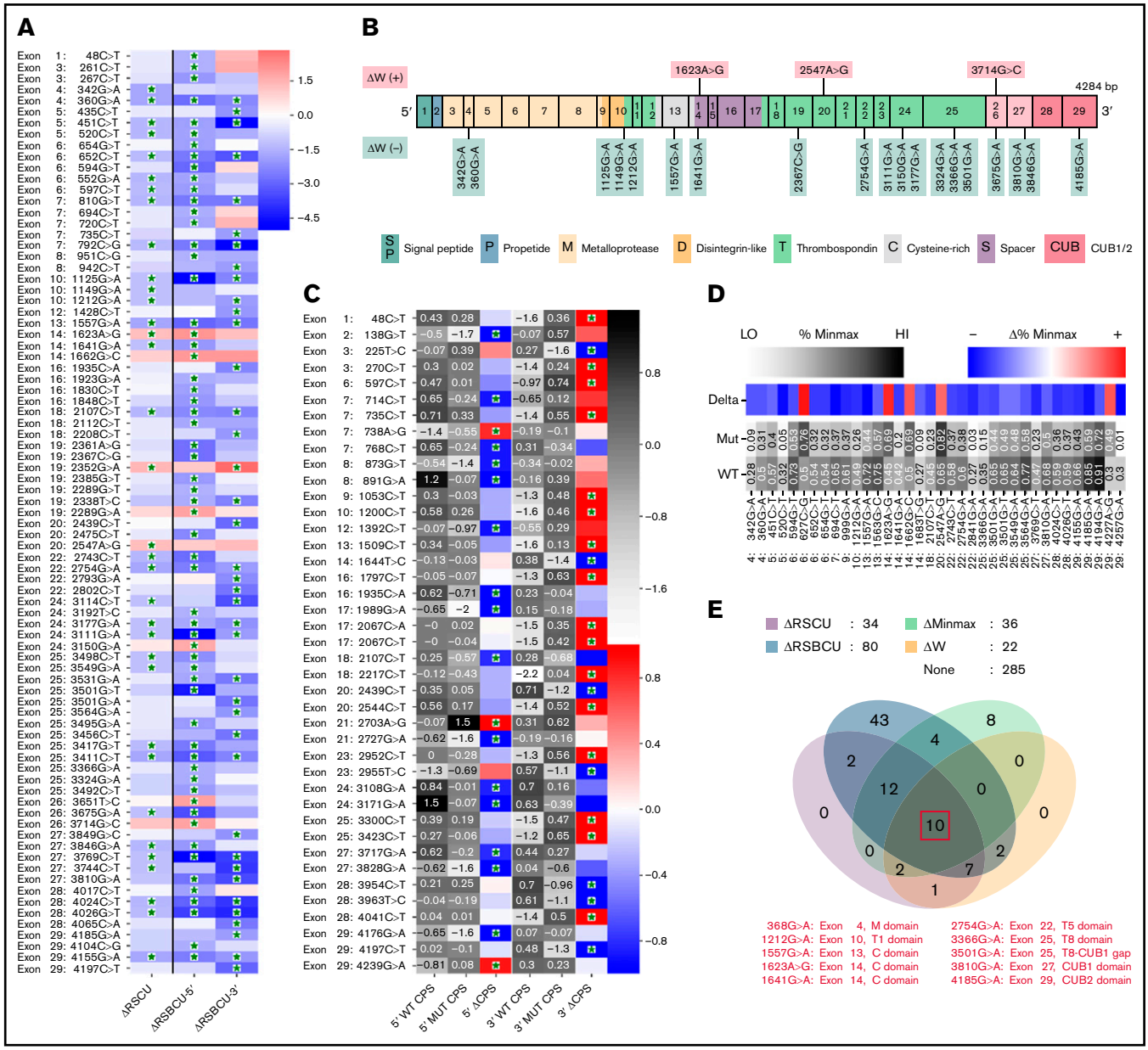

Figure 5. Synonymous variants of *ADAMTS13* affect codon usage. (A) Synonymous *ADAMTS13* variants with significantly different RSCU (ΔRSCU) or relative synonymous bicodon usage for 2 codon pairs (ΔRSBCU-5′ and ΔRSBCU-3′) compared with WT ADAMT S13. Green stars indicate significant values. (B) sSNVs with significantly different codon adaptation index (ΔW). (C) Variants with significant changes in CPS for 5′ or for 3′ codon pair. Green stars indicate whether change in CPS is significant for each variant and each codon pair. (D) Variants that result in significantly different %MinMax values. All δ values presented here are significant. (E) Overlap between variants that significantly affect ΔRSCU, relative synonymous bicodon usage ΔRS BCU, Δ%MinMax, and ΔW. Ten sSNVs that significantly affect all 4 parameters appear in red along with their exon and encoded protein domain. Differences considered significant where $P < .05$ (see the supplemental Methods for a description of *P* value computation and supplemental Excel File 1 for *P* values).

screening of sSNVs likely to affect protein properties, even for large complex genes such as *ADAMTS13*. By integrating findings from a variety of in silico tools assessing different characteristics, we can comprehensively assess multiple mechanisms by which sSNVs may exert a biological impact. Results in the current study focus on ADAMTS13 sSNVs, but our approach using in silico tools to assess several different biomolecular mechanisms is generalizable to any gene.

The estimated heritability of ADAMTS13 antigen levels suggests that most of the population variance of plasma ADAMTS13 is the result of genetic factors,[38,39] including sSNVs. Our findings suggest numerous synonymous variants that may affect ADAMTS13 properties through multiple mechanisms, including pre-mRNA splicing, miRNA silencing, and translation kinetics.

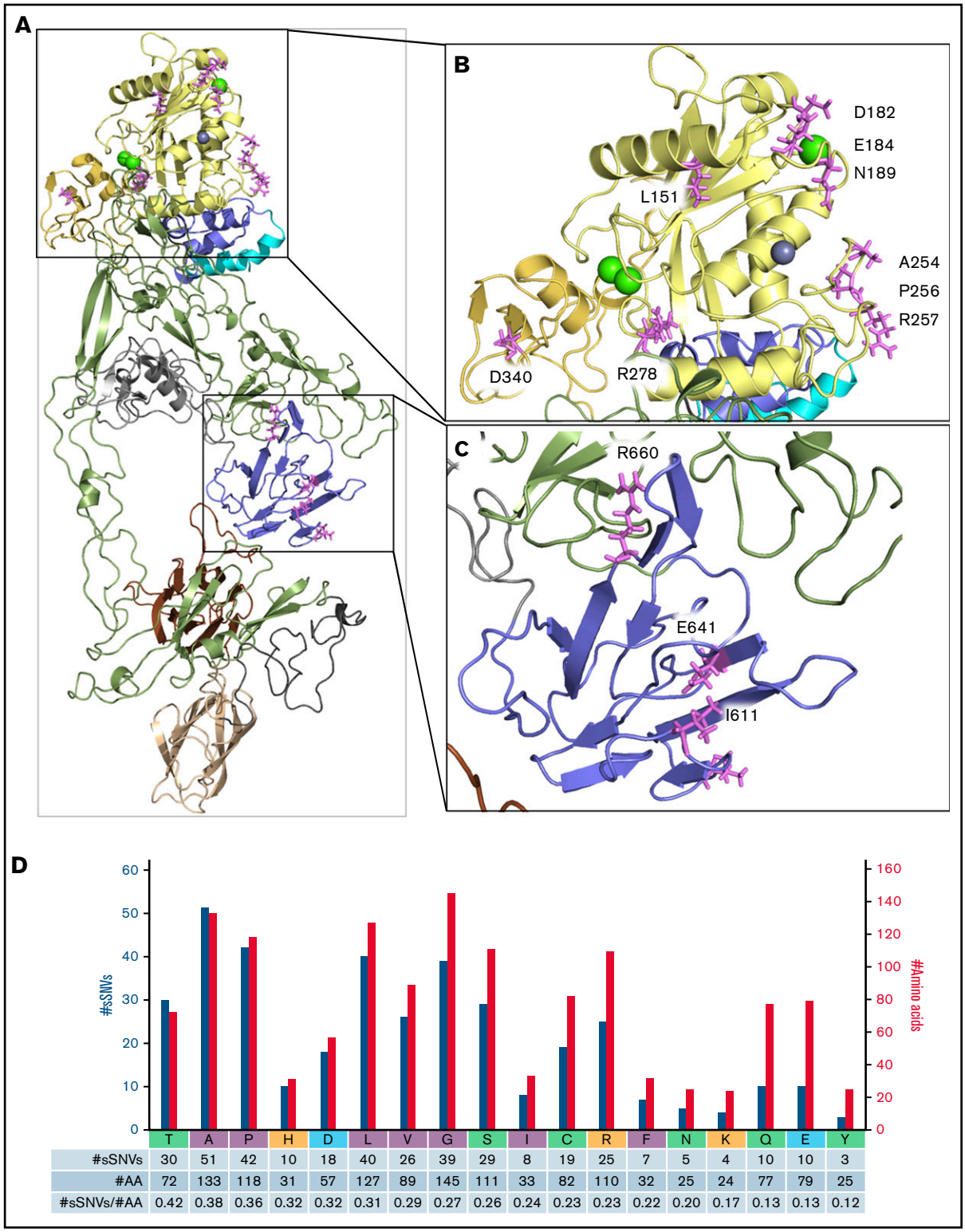

	T	A	P	H	D	L	V	G	S	I	C	R	F	N	K	Q	E	Y
#sSNVs	30	51	42	10	18	40	26	39	29	8	19	25	7	5	4	10	10	3
#AA	72	133	118	31	57	127	89	145	111	33	82	110	32	25	24	77	79	25
#sSNVs/#AA	0.42	0.38	0.36	0.32	0.32	0.31	0.29	0.27	0.26	0.24	0.23	0.23	0.22	0.20	0.17	0.13	0.13	0.12

Figure 6. *ADAMTS13* sSNVs may affect mRNA regions encoding the active site and metal-binding domains. Crystal structure of the ADAMT S13 domain (A) with the highlighted metalloprotease domain (B) and spacer domain (C) to display amino acid (AA) position that may be affected by synonymous variants of ADAMT S13. Specific ADAMT S13 domains are color coded: signal peptide = light blue; propeptide = blue; metalloprotease = yellow; disintegrin-like = gold; T1-T8 = green; C = cysteine-rich = gray; spacer = purple; CUB1 = ivory; and CUB2 = brown. (D) Number of ADAMT S13 sSNVs encoding specific amino acids (nonpolar in gray, polar in green, positively charged in red, negatively charged in blue) represented by blue bars and the number of each amino acid in ADAMT S13 represented by gold bars.

Table 3. Variants may affect ADAMTS13 protein binding or active site

sSNV	ID	Exon #	Domain	AA #	AA	Comments
451C>T	rs781937618	5	M	151	L	One of surface residues in ADAMTS13 subsite pockets localized in positions essential to accommodate VWF
546C>T (*)	rs148849381	6	M	182	D	Coordinate metal binding, in Ca-binding loop (180-193)
552G>A (*)	rs782652490	6	M	184	E	Identified in Ca-binding loop (180-193) that occlude the active-site cleft
567C>T (*)	rs782555111	6	M	189	N	Identified in Ca-binding loop (180-193) that occlude the active-site cleft
762C>T	rs1212704138	7	M	254	A	Involved in ionic interaction that bridge loops 180-193 and 231-263 that stabilized the metal-binding pocket
768C>G	rs1340581969	7	M	256	P	Stabilized subsite pocket and essential to accommodate VWF
771C>T	rs947504635	7	M	257	R	In substrate binding face in distal domain
834G>T (*)	rs587671802	8	M	278	R	In metalloprotease loop that connect distal domain and coordinate Ca-binding site
1020C>T	rs144498742	9	D	340	D	Responsible for a negative charged patch on the surface essential for electrostatic interaction with VWR
1833C>T (†)	rs1373112883	16	S	611	I	Locate within hydrophobic pocket. Part of spacer domain exosite involved in VWR binding
1860C>T	rs751652402	16	S	620	L	One of hydrophobic residues cluster on the surface. Part of spacer domain exosite involved in VWR binding
1923G>A	rs977615435	16	S	641	E	Charged residue not directed into solvent interface
1980G>A (†)	rs1397130583	17	S	660	R	Part of spacer exosite, involved in interaction between CUB essential to fold back into close conformation

Variants listed are *ADAMTS13* sSNVs that may affect protein binding or active site. Asterisks highlight sSNVs also predicted to affect mRNA splicing; daggers highlight sSNVs also predicted to affect miRNA-binding sites. AA, amino acid; D, disintegrin-like; M, metalloproteinase; S, spacer.

Although there is no single *ADAMTS13* sSNV known to be responsible for USS, there are few documented examples in the literature that associate sSNVs of *ADAMTS13* to pathologic states. In addition to USS variants (supplemental Table 1), other sSNVs has been identified and clinically evaluated (supplemental Table 7). Most of the sSNVs identified in patients with TTP have been labeled as haplotype with other synonymous variants that are associated with the disease,[15,30,83-87] and thus it is difficult to evaluate the role of sSNVs in these individuals.

The genotype analysis of *ADAMTS13* in 14 neonates diagnosed with congenital heart disease (CHD)[83] identified 4 patients with thrombosis and 10 patients without thrombosis (supplemental Table 8).[83]

Table 4. Folding energy of the nascent protein chain (F_n) for selected sSNVs

sSNV	ID	Exon	Domain	AA #	AA	F_n
999G>A	rs757725461	9	D	333	Q	−0.3902
1623A>G	rs781937390	14	C	541	V	−0.3112
2338T>C	rs782298936	19	T3	780	L	−5.919
3150G>A	rs36222579	24	T7	1050	V	−4.1288
3177G>A	rs782223782	24	T7	1059	V	−4.275
3192T>C	rs782633692	24	T7	1064	S	−0.1462
3366G>A	rs782238280	25	T8	1122	V	−0.2646
3714G>C	rs931559052	26	CUB1	1238	A	−0.3826
4024C>T	rs1044871968	28	CUB2	1342	L	−0.2598
4026G>T	rs1400291999	28	CUB2	1342	L	−0.2598

AA, amino acid; C, cysteine-rich; D, disintegrin-like.

One patient (patient 2) who developed thrombosis at the site of surgery has *ADAMTS13* haplotype with 3 sSNVs (c.420T>C [rs3118667], 1716G>A [rs372789831], c.2280T>C [rs3124767]), one not-TTP variant (c.2699C>T, rs685523), and one TPP variant (c.1370C>T, rs36220240) and was asymptomatic despite the presence of deleterious mutation previously linked to congenital TTP (c.1370C>T, rs36220240). Moreover, 10 patients with CHD exhibited high to normal ADAMTS13 antigen and activity levels (~50%, which is considered the lower normal range in neonates[88]) and have not developed thrombosis, whereas missense mutations (c.1342C>G [rs2301612, p.G448E], c.1370C>T [rs36220240, p.P457L], and c.2699C>T [rs685523, p.A900V]) often identified in patients with TTP[29,30,38] were accompanied by sSNV variants. One CHD patient (patient number 7 without thrombosis) had single sSNV: c.2280T>C (rs3124767) in the *ADAMTS13* gene and high ADAMTS13 antigen (63.6%) and activity (43.6%) levels. In addition, in vivo evaluation of the *ADAMTS13* haplotype seen in patient 2 showed that the deleterious effect seen for the TTP variant (c.1370C>T, rs36220240, p.P457L) can be rescued by synonymous variants (supplemental Table 7).[89] These studies suggest that sSNVs identified in neonates may have synergistic protective effects on ADAMTS13 functions. GWAS of plasma ADAMTS13 concentrations from healthy donors showed that individuals with c.420T>C or c.4221C>A variants exhibited ~6% increase in ADAMTS13, whereas in patients with variants c.1716G>A or c.2280 C>T, the ADAMTS13 level was ~5% lower. These synonymous variants were shown to alter ADAMTS13 expression and activity levels in in vitro studies (supplemental Tables 7 and 9).[10,41] Variant c.420T>C (rs3118667) also exhibited a 3% increase in ADAMTS13 activity by GWAS[39] and has been significantly associated with pediatric stroke.[90] In addition,

c.4221C>A was significantly more frequent in populations with major adverse cardiac events, cerebrovascular events,[91] and Thai malaria.[92]

Overall, although the effect from single sSNVs is not dramatic, coexistence of 2 or more variants may have a synergistic effect and cause significant changes in ADAMTS13 functions.[29,89,93] Combined, this evidence suggests that *ADAMTS13* sSNVs affect plasma ADAMTS13 antigen and activity levels, emphasizing their relevance to cardiovascular disease and coagulopathy.

In our in silico studies, the sSNVs identified in patient samples (supplemental Table 7) were located within RC-enriched regions (supplemental Table 9). Significantly high RC enrichment would suggest a cluster of conserved RCs around the region, thus amplifying potential impact from changes to more common codons.[94] In addition, validation of RNA minimum free energy of full-length *ADAMTS13* variants that have been identified in human subjects displayed significant differences in their RNA secondary structure (compared with WT), which may explain district antigen and activity level in those variants (supplemental Figure 2; supplemental Table 2).

To summarize, we have presented a comprehensive in silico overview of all reported *ADAMST13* sSNVs that may be used as point of reference to understand the clinical consequences of *ADAMTS13* sSNVs. We found numerous sSNVs that affect *ADAMTS13* GC content and CpG sites. Several methods were used to evaluate codon and codon pair usage changes that may affect translation rate and cotranslational folding of ADAMTS13. Moreover, our results show that 67 sSNVs confer significantly different mRNA folding energy compared with WT. Next, our analysis revealed 46 sSNVs that may affect *ADAMTS13* splicing, including two USS variants, c.936C>T (rs36219562) and c.1797C>T (rs36221216). Nine sSNVs were found that can affect the binding sites of 14 miRNAs. Although the effect of miRNA binding within coding region may not be as high as in 3′UTR, they may still contribute to observed variance in ADAMTS13 expression.[95,96]

Calculation of cotranslational folding in the nascent protein chain identified 3 variants that may substantially affect protein folding. In addition, we characterized potential effects of these sSNVs on protein structure, especially with respect to the ADAMTS13-active site.

Our previous evaluation of some *ADAMTS13* SNVs found that even the variants with moderate changes in ΔG or codon usage can affect protein properties.[10] Although further experimental evaluation is needed to fully validate the role of synonymous variation in protein function, this study has identified several *ADAMTS13* sSNVs that are most likely to affect ADAMTS13 protein properties.

Deficiency or dysfunction of ADAMTS13 can lead to thrombotic pathologies, including TTP, USS, myocardial infarction, and ischemic stroke,[18,27,97] and may contribute to COVID-19–associated coagulopathy.[20] As we show here, rare synonymous *ADAMTS13* variants may markedly contribute to the natural variation observed in the healthy population and might explain differential susceptibility to thrombosis. Most of these *ADAMTS13* sSNVs have not been identified in prior GWAS, often being systematically excluded. Better understanding of these sSNVs and appreciating how they contribute to variability in ADAMTS13 abundance and specific activity highlight the broader importance of considering sSNVs when assessing potential causes for differential gene expression, protein abundance, and structure.

Acknowledgments

The authors thank Aaron Liss, Center for Biologics Evaluation and Research, US Food and Drug Administration (CBER FDA), for his assistance gathering variants from dbSNP.

This work was supported by funds from the CBER FDA operating funds. The work was also funded by CBER FDA special COVID-19 funds.

The findings and conclusions in this article have not been formally disseminated by the FDA and should not be construed as representing any agency determination or policy.

Authorship

Contribution: K.I.J., D.M., and D.D.H. equally contributed to the manuscript and were involved in the in silico analysis, performed data analyses, and participated in writing the manuscript; J.K. performed miRNA analysis; N.H.-K. and R.C.H. assisted in the review and editing of the manuscript; U.K.K., R.C.H., and J.C.I. provided clinical data analysis; and C.K.-S. designed the research plan, oversaw the project, and wrote the manuscript.

Conflict-of-interest disclosure: The authors declare no competing financial interests.

ORCID profiles: K.I.J., 000-0002-2219-2096; D.M., 0000-0001-5148-9561; N.H.-K., 0000-0003-4954-9435; U.K.K., 0000-0002-8145-8894; C.K.-S., 0000-0002-9355-8585.

Correspondence: Chava Kimchi-Sarfaty, US Food and Drug Administration, 10903 New Hampshire Ave, Silver Spring, MD 20993; e-mail: Chava.Kimchi-Sarfaty@fda.hhs.gov.

References

1. Bali V, Bebok Z. Decoding mechanisms by which silent codon changes influence protein biogenesis and function. *Int J Biochem Cell Biol.* 2015; 64:58-74.
2. Hunt RC, Simhadri VL, Iandoli M, Sauna ZE, Kimchi-Sarfaty C. Exposing synonymous mutations. *Trends Genet.* 2014;30(7):308-321.
3. Zeng Z, Bromberg Y. Predicting functional effects of synonymous variants: a systematic review and perspectives. *Front Genet.* 2019;10:914.
4. Hamasaki-Katagiri N, Lin BC, Simon J, et al. The importance of mRNA structure in determining the pathogenicity of synonymous and non-synonymous mutations in haemophilia. *Haemophilia.* 2017;23(1):e8-e17.

5. Shabalina SA, Spiridonov NA, Kashina A. Sounds of silence: synonymous nucleotides as a key to biological regulation and complexity. *Nucleic Acids Res.* 2013;41(4):2073-2094.

6. McCarthy C, Carrea A, Diambra L. Bicodon bias can determine the role of synonymous SNPs in human diseases. *BMC Genomics.* 2017; 18(1):227.

7. Lazrak A, Fu L, Bali V, et al. The silent codon change I507-ATC->ATT contributes to the severity of the ΔF508 CFTR channel dysfunction. *FASEB J.* 2013;27(11):4630-4645.

8. Wu Q, Medina SG, Kushawah G, et al. Translation affects mRNA stability in a codon-dependent manner in human cells. *eLife.* 2019;8:8.

9. Jang HS, Shin WJ, Lee JE, Do JT. CpG and Non-CpG methylation in epigenetic gene regulation and brain function. *Genes (Basel).* 2017; 8(6):E148.

10. Edwards NC, Hing ZA, Perry A, et al. Characterization of coding synonymous and non-synonymous variants in ADAMTS13 using ex vivo and in silico approaches. *PLoS One.* 2012;7(6):e38864.

11. Tsai CJ, Sauna ZE, Kimchi-Sarfaty C, Ambudkar SV, Gottesman MM, Nussinov R. Synonymous mutations and ribosome stalling can lead to altered folding pathways and distinct minima. *J Mol Biol.* 2008;383(2):281-291.

12. Buhr F, Jha S, Thommen M, et al. Synonymous codons direct cotranslational folding toward different protein conformations. *Mol Cell.* 2016; 61(3):341-351.

13. Crawley JT, de Groot R, Xiang Y, Luken BM, Lane DA. Unraveling the scissile bond: how ADAMTS13 recognizes and cleaves von Willebrand factor. *Blood.* 2011;118(12):3212-3221.

14. Theilmeier G, Michiels C, Spaepen E, et al. Endothelial von Willebrand factor recruits platelets to atherosclerosis-prone sites in response to hypercholesterolemia. *Blood.* 2002;99(12):4486-4493.

15. Levy GG, Nichols WC, Lian EC, et al. Mutations in a member of the ADAMTS gene family cause thrombotic thrombocytopenic purpura. *Nature.* 2001;413(6855):488-494.

16. Rieger M, Mannucci PM, Kremer Hovinga JA, et al. ADAMTS13 autoantibodies in patients with thrombotic microangiopathies and other immunomediated diseases. *Blood.* 2005;106(4):1262-1267.

17. Ferrari B, Cairo A, Pagliari MT, Mancini I, Arcudi S, Peyvandi F. Risk of diagnostic delay in congenital thrombotic thrombocytopenic purpura. *J Thromb Haemost.* 2019;17(4):666-669.

18. Arning A, Hiersche M, Witten A, et al. A genome-wide association study identifies a gene network of ADAMTS genes in the predisposition to pediatric stroke. *Blood.* 2012;120(26):5231-5236.

19. Ye Z, Zheng J. Verification of the role of ADAMTS13 in the cardiovascular disease using two-sample Mendelian randomization. *Front Genet.* 2021; 12:660989.

20. Bazzan M, Montaruli B, Sciascia S, Cosseddu D, Norbiato C, Roccatello D. Low ADAMTS 13 plasma levels are predictors of mortality in COVID-19 patients. *Intern Emerg Med.* 2020;15(5):861-863.

21. Zheng X, Chung D, Takayama TK, Majerus EM, Sadler JE, Fujikawa K. Structure of von Willebrand factor-cleaving protease (ADAMTS13), a metalloprotease involved in thrombotic thrombocytopenic purpura. *J Biol Chem.* 2001;276(44):41059-41063.

22. Soejima K, Mimura N, Hirashima M, et al. A novel human metalloprotease synthesized in the liver and secreted into the blood: possibly, the von Willebrand factor-cleaving protease? *J Biochem.* 2001;130(4):475-480.

23. Akiyama M, Takeda S, Kokame K, Takagi J, Miyata T. Crystal structures of the noncatalytic domains of ADAMTS13 reveal multiple discontinuous exosites for von Willebrand factor. *Proc Natl Acad Sci U S A.* 2009;106(46):19274-19279.

24. Anderson PJ, Kokame K, Sadler JE. Zinc and calcium ions cooperatively modulate ADAMTS13 activity. *J Biol Chem.* 2006;281(2):850-857.

25. Petri A, Kim HJ, Xu Y, et al. Crystal structure and substrate-induced activation of ADAMTS13. *Nat Commun.* 2019;10(1):3781.

26. Sukumar S, Lämmle B, Cataland SR. Thrombotic thrombocytopenic purpura: pathophysiology, diagnosis, and management. *J Clin Med.* 2021; 10(3):536.

27. Alwan F, Vendramin C, Liesner R, et al. Characterization and treatment of congenital thrombotic thrombocytopenic purpura. *Blood.* 2019; 133(15):1644-1651.

28. van Dorland HA, Taleghani MM, Sakai K, et al; Hereditary TTP Registry. The International Hereditary Thrombotic Thrombocytopenic Purpura Registry: key findings at enrollment until 2017. *Haematologica.* 2019;104(10):2107-2115.

29. Plaimauer B, Fuhrmann J, Mohr G, et al. Modulation of ADAMTS13 secretion and specific activity by a combination of common amino acid polymorphisms and a missense mutation. *Blood.* 2006;107(1):118-125.

30. Kokame K, Matsumoto M, Soejima K, et al. Mutations and common polymorphisms in ADAMTS13 gene responsible for von Willebrand factor-cleaving protease activity. *Proc Natl Acad Sci U S A.* 2002;99(18):11902-11907.

31. Zheng XL. Structure-function and regulation of ADAMTS-13 protease. *J Thromb Haemost.* 2013;11(suppl 1):11-23.

32. Levy GG, Motto DG, Ginsburg D. ADAMTS13 turns 3. *Blood.* 2005;106(1):11-17.

33. Tao Z, Wang Y, Choi H, et al. Cleavage of ultralarge multimers of von Willebrand factor by C-terminal-truncated mutants of ADAMTS-13 under flow. *Blood.* 2005;106(1):141-143.

34. Shomron N, Hamasaki-Katagiri N, Hunt R, et al. A splice variant of ADAMTS13 is expressed in human hepatic stellate cells and cancerous tissues [published correction appears in *Thromb Haemost.* 2010;104(4):861]. *Thromb Haemost.* 2010;104(3):531-535.

35. Lancellotti S, De Cristofaro R. Structure and proteolytic properties of ADAMTS13, a metalloprotease involved in the pathogenesis of thrombotic microangiopathies. *Prog Mol Biol Transl Sci.* 2011;99:105-144.

36. Jiang Y, Huang D, Kondo Y, et al. Novel mutations in ADAMTS13 CUB domains cause abnormal pre-mRNA splicing and defective secretion of ADAMTS13. *J Cell Mol Med.* 2020;24(7):4356-4361.

37. Lancellotti S, Basso M, De Cristofaro R. Proteolytic processing of von Willebrand factor by ADAMTS13 and leukocyte proteases. *Mediterr J Hematol Infect Dis.* 2013;5(1):e2013058.

38. Ma Q, Jacobi PM, Emmer BT, et al. Genetic variants in *ADAMTS13* as well as smoking are major determinants of plasma ADAMTS13 levels. *Blood Adv.* 2017;1(15):1037-1046.

39. de Vries PS, Boender J, Sonneveld MA, et al. Genetic variants in the ADAMTS13 and SUPT3H genes are associated with ADAMTS13 activity. *Blood.* 2015;125(25):3949-3955.

40. Pérez-Rodríguez A, Lourés E, Rodríguez-Trillo Á, et al. Inherited ADAMTS13 deficiency (Upshaw-Schulman syndrome): a short review. *Thromb Res.* 2014;134(6):1171-1175.

41. Hunt R, Hettiarachchi G, Katneni U, et al. A single synonymous variant (c.354G>A [p.P118P]) in *ADAMTS13* confers enhanced specific activity. *Int J Mol Sci.* 2019;20(22):E5734.

42. Zuker M. Mfold web server for nucleic acid folding and hybridization prediction. *Nucleic Acids Res.* 2003;31(13):3406-3415.

43. Zadeh JN, Steenberg CD, Bois JS, et al. NUPACK: analysis and design of nucleic acid systems. *J Comput Chem.* 2011;32(1):170-173.

44. Xayaphoummine A, Bucher T, Isambert H. Kinefold web server for RNA/DNA folding path and structure prediction including pseudoknots and knots. Nucleic Acids Res. 2005;33(web server issue):W605-W610.

45. Salari R, Kimchi-Sarfaty C, Gottesman MM, Przytycka TM. Sensitive measurement of single-nucleotide polymorphism-induced changes of RNA conformation: application to disease studies. *Nucleic Acids Res.* 2013;41(1):44-53.

46. Hofacker IL. Vienna RNA secondary structure server. *Nucleic Acids Res.* 2003;31(13):3429-3431.

47. Yeo G, Burge CB. Maximum entropy modeling of short sequence motifs with applications to RNA splicing signals. *J Comput Biol.* 2004; 11(2-3):377-394.

48. Reese MG, Eeckman FH, Kulp D, Haussler D. Improved splice site detection in Genie. *J Comput Biol.* 1997;4(3):311-323.

49. Shapiro MB, Senapathy P. RNA splice junctions of different classes of eukaryotes: sequence statistics and functional implications in gene expression. *Nucleic Acids Res.* 1987;15(17):7155-7174.

50. Pertea M, Lin X, Salzberg SL. GeneSplicer: a new computational method for splice site prediction. *Nucleic Acids Res.* 2001;29(5):1185-1190.

51. Wong N, Wang X. miRDB: an online resource for microRNA target prediction and functional annotations. *Nucleic Acids Res.* 2015;43(database issue):D146-D152.

52. Chen Y, Wang X. miRDB: an online database for prediction of functional microRNA targets. *Nucleic Acids Res.* 2020;48(D1):D127-D131.

53. Šulc M, Marín RM, Robins HS, Vaníček J. PACCMIT/PACCMIT-CDS: identifying microRNA targets in 3′ UTRs and coding sequences. *Nucleic Acids Res.* 2015;43(W1):W474-W479.

54. Marín RM, Sulc M, Vanícek J. Searching the coding region for microRNA targets. *RNA.* 2013;19(4):467-474.

55. Lewis BP, Shih IH, Jones-Rhoades MW, Bartel DP, Burge CB. Prediction of mammalian microRNA targets. *Cell.* 2003;115(7):787-798.

56. Sharp PM, Li WH. The codon Adaptation Index–a measure of directional synonymous codon usage bias, and its potential applications. *Nucleic Acids Res.* 1987;15(3):1281-1295.

57. Coleman JR, Papamichail D, Skiena S, Futcher B, Wimmer E, Mueller S. Virus attenuation by genome-scale changes in codon pair bias. *Science.* 2008;320(5884):1784-1787.

58. Jacobs WM, Shakhnovich EI. Evidence of evolutionary selection for cotranslational folding. *Proc Natl Acad Sci U S A.* 2017;114(43):11434-11439.

59. Rodriguez A, Wright G, Emrich S, Clark PL. %MinMax: a versatile tool for calculating and comparing synonymous codon usage and its impact on protein folding. *Protein Sci.* 2018;27(1):356-362.

60. Zhang D, Xia J. Somatic synonymous mutations in regulatory elements contribute to the genetic aetiology of melanoma. *BMC Med Genomics.* 2020;13(suppl 5):43.

61. Bin Y, Wang X, Zhao L, Wen P, Xia J. An analysis of mutational signatures of synonymous mutations across 15 cancer types. *BMC Med Genet.* 2019;20(suppl 2):190.

62. Piovesan A, Antonaros F, Vitale L, Strippoli P, Pelleri MC, Caracausi M. Human protein-coding genes and gene feature statistics in 2019. *BMC Res Notes.* 2019;12(1):315.

63. Shen H, Li J, Zhang J, et al. Comprehensive characterization of human genome variation by high coverage whole-genome sequencing of forty four Caucasians. *PLoS One.* 2013;8(4):e59494.

64. Kertesz M, Wan Y, Mazor E, et al. Genome-wide measurement of RNA secondary structure in yeast. *Nature.* 2010;467(7311):103-107.

65. Chamary JV, Hurst LD. Evidence for selection on synonymous mutations affecting stability of mRNA secondary structure in mammals. *Genome Biol.* 2005;6(9):R75.

66. Nackley AG, Shabalina SA, Tchivileva IE, et al. Human catechol-O-methyltransferase haplotypes modulate protein expression by altering mRNA secondary structure. *Science.* 2006;314(5807):1930-1933.

67. Moore LD, Le T, Fan G. DNA methylation and its basic function. *Neuropsychopharmacology.* 2013;38(1):23-38.

68. Brenet F, Moh M, Funk P, et al. DNA methylation of the first exon is tightly linked to transcriptional silencing. *PLoS One.* 2011;6(1):e14524.

69. Wang Y, Qiu C, Cui Q. A large-scale analysis of the relationship of synonymous SNPs changing microRNA regulation with functionality and disease. *Int J Mol Sci.* 2015;16(10):23545-23555.

70. Wang Y, Yu D, Tolleson WH, et al. A systematic evaluation of microRNAs in regulating human hepatic CYP2E1. *Biochem Pharmacol.* 2017;138: 174-184.

71. Kiener M, Chen L, Krebs M, et al. miR-221-5p regulates proliferation and migration in human prostate cancer cells and reduces tumor growth in vivo. *BMC Cancer.* 2019;19(1):627.

72. Zhou W, Inada M, Lee TP, et al. ADAMTS13 is expressed in hepatic stellate cells. *Lab Invest.* 2005;85(6):780-788.

73. Markovic J, Sharma AD, Balakrishnan A. MicroRNA-221: a fine tuner and potential biomarker of chronic liver injury. *Cells.* 2020;9(8):E1767.

74. Fu Y, Liu M, Li F, et al. MiR-221 promotes hepatocellular carcinoma cells migration via targeting PHF2. *BioMed Res Int.* 2019;2019:4371405.

75. Clarke TF IV, Clark PL. Rare codons cluster. *PLoS One.* 2008;3(10):e3412.

76. Komar AA. A code within a code: how codons fine-tune protein folding in the cell. *Biochemistry (Mosc).* 2021;86(8):976-991.

77. Peterson J, Li S, Kaltenbrun E, Erdogan O, Counter CM. Expression of transgenes enriched in rare codons is enhanced by the MAPK pathway. *Sci Rep.* 2020;10(1):22166.

78. Pos W, Crawley JT, Fijnheer R, Voorberg J, Lane DA, Luken BM. An autoantibody epitope comprising residues R660, Y661, and Y665 in the ADAMTS13 spacer domain identifies a binding site for the A2 domain of VWF. *Blood.* 2010;115(8):1640-1649.

79. Jin SY, Skipwith CG, Zheng XL. Amino acid residues Arg(659), Arg(660), and Tyr(661) in the spacer domain of ADAMTS13 are critical for cleavage of von Willebrand factor. *Blood.* 2010;115(11):2300-2310.

80. South K, Luken BM, Crawley JT, et al. Conformational activation of ADAMTS13. *Proc Natl Acad Sci U S A.* 2014;111(52):18578-18583.

81. Zhou Z, Yeh HC, Jing H, et al. Cysteine residues in CUB-1 domain are critical for ADAMTS13 secretion and stability. *Thromb Haemost.* 2011; 105(1):21-30.

82. Melnikov S, Mailliot J, Rigger L, et al. Molecular insights into protein synthesis with proline residues. *EMBO Rep.* 2016;17(12):1776-1784.

83. Katneni UK, Holcomb DD, Hernandez NE, et al. In silico features of ADAMTS13 contributing to plasmatic ADAMTS13 levels in neonates with congenital heart disease. *Thromb Res.* 2020;193:66-76.

84. Kim B, Hing ZA, Wu A, et al. Single-nucleotide variations defining previously unreported ADAMTS13 haplotypes are associated with differential expression and activity of the VWF-cleaving protease in a Salvadoran congenital thrombotic thrombocytopenic purpura family. *Br J Haematol.* 2014;165(1):154-158.

85. Matsumoto M, Kokame K, Soejima K, et al. Molecular characterization of ADAMTS13 gene mutations in Japanese patients with Upshaw-Schulman syndrome. *Blood.* 2004;103(4):1305-1310.

86. Ma E, Li YH, Kwok J, Ling SC, Yau PW, Chan GCF. ADAMTS13 mutational analysis in Chinese patients with chronic relapsing thrombotic thrombocytopenic purpura. *Hong Kong J Paediatr.* 2006;11(1):22-27.

87. Fujimura Y, Matsumoto M, Kokame K, et al. Pregnancy-induced thrombocytopenia and TTP, and the risk of fetal death, in Upshaw-Schulman syndrome: a series of 15 pregnancies in 9 genotyped patients. *Br J Haematol.* 2009;144(5):742-754.

88. Katneni UK, Ibla JC, Hunt R, Schiller T, Kimchi-Sarfaty C. von Willebrand factor/ADAMTS-13 interactions at birth: implications for thrombosis in the neonatal period. *J Thromb Haemost.* 2019;17(3):429-440.

89. Katneni UK, Hunt R, Hettiarachchi GK, Hamasaki-Katagiri N, Kimchi-Sarfaty C, Ibla JC. Compounding variants rescue the effect of a deleterious ADAMTS13 mutation in a child with severe congenital heart disease. *Thromb Res.* 2017;158:98-101.

90. Stoll M, Rühle F, Witten A, et al. Rare variants in the ADAMTS13 von Willebrand factor-binding domain contribute to pediatric stroke. *Circ Cardiovasc Genet.* 2016;9(4):357-367.

91. Liu R, Song L, Jiang L, et al. Susceptible gene polymorphism in patients with three-vessel coronary artery disease. *BMC Cardiovasc Disord.* 2020; 20(1):172.

92. Kraisin S, Naka I, Patarapotikul J, et al. Association of ADAMTS13 polymorphism with cerebral malaria. *Malar J.* 2011;10(1):366.

93. Zheng L, Zhang D, Cao W, Song WC, Zheng XL. Synergistic effects of ADAMTS13 deficiency and complement activation in pathogenesis of thrombotic microangiopathy. *Blood.* 2019;134(13):1095-1105.

94. Chaney JL, Steele A, Carmichael R, et al. Widespread position-specific conservation of synonymous rare codons within coding sequences. *PLOS Comput Biol.* 2017;13(5):e1005531.

95. Forman JJ, Coller HA. The code within the code: microRNAs target coding regions. *Cell Cycle.* 2010;9(8):1533-1541.

96. Fang Z, Rajewsky N. The impact of miRNA target sites in coding sequences and in 3'UTRs. *PLoS One.* 2011;6(3):e18067.

97. Tsai HM. Advances in the pathogenesis, diagnosis, and treatment of thrombotic thrombocytopenic purpura. *J Am Soc Nephrol.* 2003;14(4):1072-1081.